



Year: 2023

Combined inhibition of BCL-2 and MCL-1 overcomes BAX deficiency-mediated resistance of TP53-mutant acute myeloid leukemia to individual BH3 mimetics

Carter, Bing Z ; Mak, Po Yee ; Tao, Wenjing ; Ayoub, Edward ; Ostermann, Lauren B ; Huang, Xuelin ; Loghavi, Sanam ; Boettcher, Steffen ; Nishida, Yuki ; Ruvolo, Vivian ; Hughes, Paul E ; Morrow, Phuong K ; Haferlach, Torsten ; Kornblau, Steven ; Muftuoglu, Muharrem ; Andreeff, Michael

Abstract: TP53-mutant acute myeloid leukemia (AML) respond poorly to currently available treatments, including venetoclax-based drug combinations and pose a major therapeutic challenge. Analyses of RNA sequencing and reverse phase protein array datasets revealed significantly lower BAX RNA and protein levels in TP53-mutant compared to TP53-wild-type (WT) AML, a finding confirmed in isogenic CRISPR-generated TP53-knockout and -mutant AML. The response to either BCL-2 (venetoclax) or MCL-1 (AMG176) inhibition was BAX-dependent and much reduced in TP53-mutant compared to TP53-WT cells, while the combination of two BH3 mimetics effectively activated BAX, circumventing survival mechanisms in cells treated with either BH3 mimetic, and synergistically induced cell death in TP53-mutant AML and stem/progenitor cells. The BH3 mimetic-driven stress response and cell death patterns after dual inhibition were largely independent of TP53 status and affected by apoptosis induction. Co-targeting, but not individual targeting of BCL-2 and MCL-1 in mice xenografted with TP53-WT and TP53-R248W Molm13 cells suppressed both TP53-WT and TP53-mutant cell growth and significantly prolonged survival. Our results demonstrate that co-targeting BCL-2 and MCL-1 overcomes BAX deficiency-mediated resistance to individual BH3 mimetics in TP53-mutant cells, thus shifting cell fate from survival to death in TP53-deficient and -mutant AML. This concept warrants clinical evaluation.

DOI: <https://doi.org/10.1038/s41408-023-00830-w>

Posted at the Zurich Open Repository and Archive, University of Zurich

ZORA URL: <https://doi.org/10.5167/uzh-239029>

Journal Article

Published Version



The following work is licensed under a Creative Commons: Attribution 4.0 International (CC BY 4.0) License.

Originally published at:








Carter, Bing Z; Mak, Po Yee; Tao, Wenjing; Ayoub, Edward; Ostermann, Lauren B; Huang, Xuelin; Loghavi, Sanam; Boettcher, Steffen; Nishida, Yuki; Ruvolo, Vivian; Hughes, Paul E; Morrow, Phuong K; Haferlach, Torsten; Kornblau, Steven; Muftuoglu, Muharrem; Andreeff, Michael (2023). Combined inhibition of BCL-2 and MCL-1 overcomes BAX deficiency-mediated resistance of TP53-mutant acute myeloid leukemia to individual BH3 mimetics. *Blood Cancer Journal*, 13(1):57.

DOI: <https://doi.org/10.1038/s41408-023-00830-w>

ARTICLE OPEN



Combined inhibition of BCL-2 and MCL-1 overcomes BAX deficiency-mediated resistance of *TP53*-mutant acute myeloid leukemia to individual BH3 mimetics

Bing Z. Carter¹ , Po Yee Mak¹, Wenjing Tao¹, Edward Ayoub¹, Lauren B. Ostermann¹ , Xuelin Huang², Sanam Loghavi³ , Steffen Boettcher⁴ , Yuki Nishida¹, Vivian Ruvolo¹, Paul E. Hughes⁵, Phuong K. Morrow⁶, Torsten Haferlach⁷ , Steven Kornblau¹ , Muharrem Muftuoglu¹ and Michael Andreeff¹ 

© The Author(s) 2023, corrected publication 2023

TP53-mutant acute myeloid leukemia (AML) respond poorly to currently available treatments, including venetoclax-based drug combinations and pose a major therapeutic challenge. Analyses of RNA sequencing and reverse phase protein array datasets revealed significantly lower BAX RNA and protein levels in *TP53*-mutant compared to *TP53*-wild-type (WT) AML, a finding confirmed in isogenic CRISPR-generated *TP53*-knockout and -mutant AML. The response to either BCL-2 (venetoclax) or MCL-1 (AMG176) inhibition was BAX-dependent and much reduced in *TP53*-mutant compared to *TP53*-WT cells, while the combination of two BH3 mimetics effectively activated BAX, circumventing survival mechanisms in cells treated with either BH3 mimetic, and synergistically induced cell death in *TP53*-mutant AML and stem/progenitor cells. The BH3 mimetic-driven stress response and cell death patterns after dual inhibition were largely independent of *TP53* status and affected by apoptosis induction. Co-targeting, but not individual targeting of BCL-2 and MCL-1 in mice xenografted with *TP53*-WT and *TP53*-R248W Molm13 cells suppressed both *TP53*-WT and *TP53*-mutant cell growth and significantly prolonged survival. Our results demonstrate that co-targeting BCL-2 and MCL-1 overcomes BAX deficiency-mediated resistance to individual BH3 mimetics in *TP53*-mutant cells, thus shifting cell fate from survival to death in *TP53*-deficient and -mutant AML. This concept warrants clinical evaluation.

Blood Cancer Journal (2023)13:57; <https://doi.org/10.1038/s41408-023-00830-w>

INTRODUCTION

Patients with *TP53*-mutant acute myeloid leukemia (AML) respond poorly to current therapies. Consequently, *TP53* mutations are frequently enriched/selected in refractory/relapsed AML [1–4], and associated with low survival rates [5–8].

The combination of the BCL-2 inhibitor venetoclax (VEN) with a hypomethylating agent (HMA) or low-dose Ara-C elicits complete remission/complete remission with incomplete hematologic recovery rates of >65%, is well tolerated by elderly AML patients [9, 10], and has been approved by the US Food and Drug Administration. This combination has also shown promising results in refractory/relapsed AML [11]. Apoptosis induction depends highly on intact p53 signaling [12]. Not surprisingly, patients with *TP53* mutations have vastly inferior responses to VEN-based therapies [13–16], supported by a recent pre-clinical study demonstrating that *TP53* mutations confer resistance to HMA/VEN in vitro and in vivo [17] and CRISPR genome editing analyses demonstrating that the loss of p53-regulated apoptosis networks confers resistance of AML cells to VEN [18]. Furthermore, a retrospective analysis showed that adding VEN to standard therapies does not improve the outcomes of patients with *TP53*-mutant AML [19].

Mitochondria-mediated apoptosis is controlled by pro- and anti-apoptotic BCL-2 proteins. We and others have reported that MCL-1, a major resistance factor for BCL-2 inhibition, is frequently induced in VEN-resistant AML cells [20–22] and that co-inhibition of BCL-2 and MCL-1 is highly synergistic, both in vitro and in vivo, against various malignant cells, including AML cells and stem/progenitor cells, that have intrinsic or acquired resistance to VEN [18, 23–28]. In addition, *BAX* mutations can confer VEN resistance to AML cells [29]. We reported that combined p53 activation and BCL-2 inhibition is synthetically lethal in *TP53*-WT AML by promoting pro-apoptotic BCL-2 proteins and targeting MCL-1 [21]. We, therefore, postulated that directly targeting MCL-1 may partially compensate for p53 deficiency and enhance VEN activity in *TP53*-mutant AML.

Alterations in the balance of pro- and anti-apoptotic BCL-2 proteins could restrict the response of *TP53*-mutant cells to BH3 mimetics. We determined RNA and protein levels of BCL-2 family members in large cohorts of *TP53*-mutant AML and investigated if shifting the balance of BCL-2 proteins to pro-death by co-targeting BCL-2 and MCL-1 could overcome *TP53*-mutant AML resistance to individual BH3 mimetics. We here report that

¹Section of Molecular Hematology and Therapy, Department of Leukemia, The University of Texas MD Anderson Cancer Center, Houston, TX, USA. ²Department of Biostatistics, The University of Texas MD Anderson Cancer Center, Houston, TX, USA. ³Department of Hematopathology, The University of Texas MD Anderson Cancer Center, Houston, TX, USA. ⁴Department of Medical Oncology and Hematology, University Hospital Zurich and University of Zurich, Zurich, Switzerland. ⁵Oncology Research, Amgen Inc, Thousand Oaks, CA, USA. ⁶Amgen Inc, Thousand Oaks, CA, USA. ⁷MLL Munich Leukemia Laboratory, Munich, Germany. [✉]email: bicarter@mdanderson.org; mandreeff@mdanderson.org

Received: 13 December 2022 Revised: 7 March 2023 Accepted: 4 April 2023

Published online: 24 April 2023

Table 1. Patient characteristics.

Patient no.	Blast %	TP53 mutations (VAF%)	Other mutations	Previous treatments and responses
26	50	c.659 A > G p.Y220C (15) c.427 G > A p.V143M (14)	NF1, PTPN11, NRAS, KRAS	Resistance to rituximab, palbociclib, and fluvestrant
28	95	c.733 G > A p.G245S (87)	NF1, TET2, DNMT3A	Resistance/relapsed AML. Resistance to chemotherapy and to VEN-based therapy
29	89	c.403 T > G p.C135G (86)	NF1, DNMT3A	Resistance/relapsed AML. Resistance to azacitidine/VEN, and BP1001 + decitabine
30	85	c.994-1 G > A (70)	NF1, ASXL1, CEBPA, KDM6A, RUNX1	Resistance/relapsed AML. Resistance to 7 + 3, fludarabine- idarubicin-VEN, PLX51107 + azacitidine, daratumumab + VEN
32	88	c.742 C > T p.R248W (80)		Resistance to cladribine and low-dose cytarabine, azacitidine, VEN and pevonedistat, PLX51107 + azacitidine.
33	65	c.517 G > A p.V173M (46) c.376-1 G > A (43)		Resistance to azacitidine
34	94	c.814 G > A p.V272M (22) c.537 T > A p.H179Q (25)	ASXL1, CEBPA	Newly diagnosed
35	78	c.445dup p.S149fs (89)	BCOR, TET2, IDH2, STAG2, DNMT3A	Refractory AML. Resistance to fludarabine, cytarabine, filgrastim, idarubicin, VEN, 5-azacitidine plus VEN, LY3410738.

decreased expression of BAX in TP53-defective AML cells contributes to their resistance to BH3 mimetics. Co-targeting of BCL-2 and MCL-1 overcomes BAX deficiency-mediated resistance of TP53-mutant AML and AML stem/progenitor cells to individual BH3 mimetics in vitro and in xenografts comprising both TP53-WT and -mutant Molm13 cells in vivo.

MATERIALS AND METHODS

Cells, cell culture, and treatment

Molm13 cells were purchased from the German Collection of Microorganisms and Cell Cultures (Braunschweig, Germany). U937, KG1, and THP1 cells were purchased from ATCC (Manassas, VA). Cell lines were validated by STR DNA fingerprinting using the AmpF_STR Identifier kit according to the manufacturer's instructions (Applied Biosystems). The STR profiles were compared to known ATCC fingerprints, and to the Cell Line Integrated Molecular Authentication database (CLIMA) version 0.1.200808 (<http://bioinformatics.istge.it/clima/>) [30]. The STR profiles matched known DNA fingerprints or were identified as unique. Mycoplasma was tested with Detection Kit from Applied Biological Materials (Richmond, BC, Canada) per the manufacturer's instructions. TP53-R248W Molm13 [31] and TP53-knockout (KO) and -mutant (R175H, Y220C, M237I, R248Q, R273H, and R282W) Molm13 cells [32] were generated as described previously. BAX-knockdown (KD) and vector control Molm13 cells [33] and p53-KD and control OCI-AML3 cells [34] were generated as described previously. Primary AML peripheral blood samples with TP53 mutations were obtained from patients (Table 1) after obtaining written informed consent following protocols approved by MD Anderson Cancer Center Institutional Review Board and in accordance with the Declaration of Helsinki. Human bone marrow (BM)-derived mesenchymal stromal cells (MSCs) were isolated from normal donors as described previously [35]. Cell lines and mononuclear cells from primary samples were cultured under previously described conditions [28]. AML cell lines without and primary cells with MSC co-cultures (4:1 ratio) were treated with DMSO, VEN, AMG176, or the combination.

Generation of VEN and AMG176-resistant cells

To generate AML cells with acquired resistance to both BCL-2 and MCL-1 inhibitors, we treated MV4-11 cells with acquired resistance to VEN previously generated [21] with increasing concentrations of AMG176 over a period of ~2 months.

RNA-seq analysis

We performed differential gene expression analysis between TP53-mutant ($n = 63$) and -WT ($n = 668$) AML patient samples collected at diagnosis using a dataset from Dr. Torsten Haferlach, MLL Munich Leukemia Laboratory, and the Torsten Haferlach Leukemia Diagnostic Foundation, Munich, Germany. These sample sizes are sufficient to provide 99% power

for a 0.5 log fold change, with the false discovery rate being controlled under 5%.

Reverse phase protein array

Proteomic profiling of >200 proteins in samples obtained from newly diagnosed AML patients were performed by reverse phase protein arrays (RPPA) following the custom-built AML array [36–38]. Among these samples, 122 were from de novo AML patients with known TP53 gene status, who had not been exposed to chemotherapy. The log₂-normalized expression levels of BCL-2 family proteins in this cohort were analyzed and compared between the TP53-WT ($n = 101$) and -mutant ($n = 21$) samples. These sample sizes are sufficient to provide 90% power for a 0.5 log fold change, with the false discovery rate being controlled under 5%.

Cell viability assay

Viable cell numbers and apoptosis were determined by flow cytometry as previously described [28]. For primary samples co-cultured with MSCs, Annexin positivity was determined in bulk (CD45⁺), and leukemia stem/progenitor cells (CD34⁺) and expressed as specific apoptosis [22, 39]:

$$\frac{\% \text{ of apoptosis in treated cells} - \% \text{ of apoptosis in untreated cells}}{\% \text{ of viable untreated cells}} \times 100\%$$

Western blot

Western blot was carried out and analyzed as described previously [27] using the Odyssey Infrared Imaging System for signal detection and Odyssey software version 3.0 for quantification (LI-COR Biosciences; Lincoln, NE). Antibodies against BCL-2 (#M088729-2) were purchased from Dako/Agilent (Santa Clara, CA); against BCL-2A1 (#14093), BCL-XL (#2764), MCL-1 (#94296), and BID (#8762), from Cell Signaling Technology (Danvers, MA); against BAX (#B8554), from Sigma; against BIM (#ab32158), NOXA (#ab13654), and PUMA (#ab186917), from Abcam (Cambridge, MA); against BAK (#NBP1-74026), from Novus Biologicals (Centennial, CO); and against p53 (DO-1) (#sc-126), from Santa Cruz Biotechnology, Inc. (Dallas, TX). β -actin was used as a loading control.

BAX and BAK activation assay

Activation of BAX and BAK was determined following the described assay [40]. Antibodies against BAX (clone 6A7) (#556467) and BAK (#556382) were purchased from BD Biosciences, San Diego, CA. Cytochrome C (#612310) (BioLegend, San Diego, CA) release was determined concomitantly to assess loss in mitochondrial membrane potential.

Multi-modality cell death assay

Cell fates were determined using a multi-metric cell death assay [41], modified from a previously described assay [42]. Briefly, cells were stained

with a live/dead cell dye (Tonbo Biosciences, San Diego, CA); fixed and permeabilized; stained with antibodies against various cell death and survival markers, including ATF4 (#10835-1-AP) (Proteintech, IL), p21 (#5487 S) (Cell Signaling Technology), RIP3 (#sc-374639) (Santa Cruz Biotechnology, Inc.), γ -H2AX (#613420) (BioLegend), Ki-67 (#563756) (BD Biosciences), LC3B (#8899) (Cell Signaling Technology), and cleaved-caspase 3 (#560627) and cleaved-PARP (#564130) (both from BD Biosciences); and subjected to flow cytometric analysis. The percentages of dead cells and cleaved-caspase 3 or cleaved-PARP positive cells among all cells were calculated, and the geometric means (G-means) of ATF4, p21, RIP3, γ -H2AX, Ki-67, and LC3B in the live cells were determined. Data were expressed as UMAP plots and heatmaps. Prior to performing high-dimensional analysis, we excluded debris, gated on singlets, and exported events, including both live and dead cells, for downstream analysis. Pooled cells from all the experimental conditions were subjected to UMAP dimension reduction and FlowSOM clustering (Omiq.ai). Arcsinh-transformed or scaled median signal intensities were used to generate heatmaps or data plots in R software version 3.6.3 (R Foundation for Statistical Computing, Vienna, Austria; <https://www.R-project.org>) as described previously [43]. The Seurat package [44] was used to cluster *TP53*-WT, -deficient, and -mutant (R175H and R248Q) leukemia cells treated with DMSO, VEN, AMG176, or both based on the expression levels of the features assessed using flow cytometry. UMAP embedding based on 4 principal components was used to separate different experimental conditions.

In vivo experiments

Mouse experiments were conducted in accordance with MD Anderson's Institutional Animal Care and Use Committee-approved protocols. Molm13 cells (0.30×10^6 luciferase/GFP-labeled *TP53*-WT plus 0.03×10^6 BFP-labeled *TP53*-R248W cells) were injected into the tail veins of 6- to 8-week-old male NSG mice (strain-005557, The Jackson Laboratory, Sacramento, CA). Once engraftment was confirmed by luciferase imaging with the IVIS-200 noninvasive bioluminescence in vivo imaging system (Xenogen, Hopkinton, MA), mice (5 or 6/group) were treated with vehicle (25% hydroxypropyl- β -cyclodextrin, pH 9), VEN (50 mg/kg, 6-day on/1-day off), AMG176 (30 mg/kg, day-2 and day-3 of each week), or VEN and AMG176 combination. Both agents were provided by Amgen and given via oral gavage. Disease progression and treatment responses were monitored with luciferase imaging and flow cytometric measurement of circulating GFP- and BFP-positive cells on day-3 of each week. Mouse survival was followed.

Statistical analyses

Cell line experiments were performed in independent triplicates; results were expressed as means \pm SEMs. The Student *t*-test was used to assess differences between groups. All tests are two-sided and *P* values ≤ 0.05 were considered statistically significant. Multiple testing was adjusted by the Benjamini–Hochberg procedure so that the resulting false discovery rate would be ≤ 0.05 . These analyses were performed using the publicly available software package limma (<https://bioconductor.org/packages/release/bioc/html/limma.html>). The combination index (CI) [45], determined using Calcsyn software, was expressed as mean CI values at ED₅₀, ED₇₅, and ED₉₀. A CI <1 indicates synergistic; CI = 1, additive; and CI >1, antagonistic effects. The Kaplan–Meier method was used to estimate mouse survival, and survival data were analyzed using the log-rank test.

RESULTS

BAX expression is significantly decreased in *TP53*-mutant AML cells

To understand the potential mechanisms underlying resistance to VEN-based therapies in *TP53*-mutant AML, we first assessed the expression of BCL-2 proteins in AML. RNA-seq analysis compared the expression of BCL-2 family members in *TP53*-mutant ($n = 63$; VAF = 4.46 to 99.2%; distribution shown in supplemental Fig. 1) with *TP53* WT ($n = 668$) samples at diagnosis. The volcano plot, generated using the ggplot2 package in R, has a *P* cutoff of 0.5 Log₂ fold change (FC) and 0.05 of adjusted *P* value cutoff (Fig. 1A). Highlighted are *TP53* and the differentially expressed BCL-2-related genes. Although none of the BCL-2 members made

the *P* cutoff of 0.5 Log₂FC, significant decreases in BAX and BCL-2 and increases in BCL-2L1 (BIM), BAD, and BBC3 (PUMA) were observed (adjust *P* < 0.05) (Fig. 1A). We next analyzed the levels of various BCL-2 proteins using an RPPA dataset generated from a large cohort of newly diagnosed de novo AML patients with known *TP53* genotype status ($n = 122$). As expected, p53 protein levels were significantly higher in *TP53*-mutant ($n = 21$) than in *TP53*-WT AML ($n = 101$; *P* < 0.001). *TP53* VAFs were not available and could vary greatly among these samples. Even so, we found that only the BAX levels were significantly lower in *TP53*-mutant than in *TP53*-WT AML (*P* = 0.006) among BCL-2 family proteins (Fig. 1B and Supplemental Fig. 2).

To validate that *TP53*-deficiency is indeed responsible for BAX reduction, we determined the expression of BCL-2 proteins in isogenic Molm13 cells with *TP53*-WT, *TP53*-KO, or various *TP53* hotspot mutations [32]. Compared with WT controls, *TP53*-defective cells show variably altered expression of various BCL-2 proteins. Among them, BAX is markedly decreased in *TP53*-KO/mutant cells (Fig. 1C), and it is the only BCL-2 protein significantly decreased in all *TP53*-deficient cells compared to controls (*P* = 0.03–0.0003). Interestingly, in addition to increased MCL-1, we recently reported that AML cells with acquired resistance to VEN or to AMG176 had decreased BAX [28]. These results suggest that BAX reduction contributes to BH3 mimetic resistance in *TP53*-deficient AML cells.

Co-targeting BCL-2 and MCL-1 overcomes BAX-dependent decreased sensitivity of *TP53*-mutant AML cells to BH3 mimetics

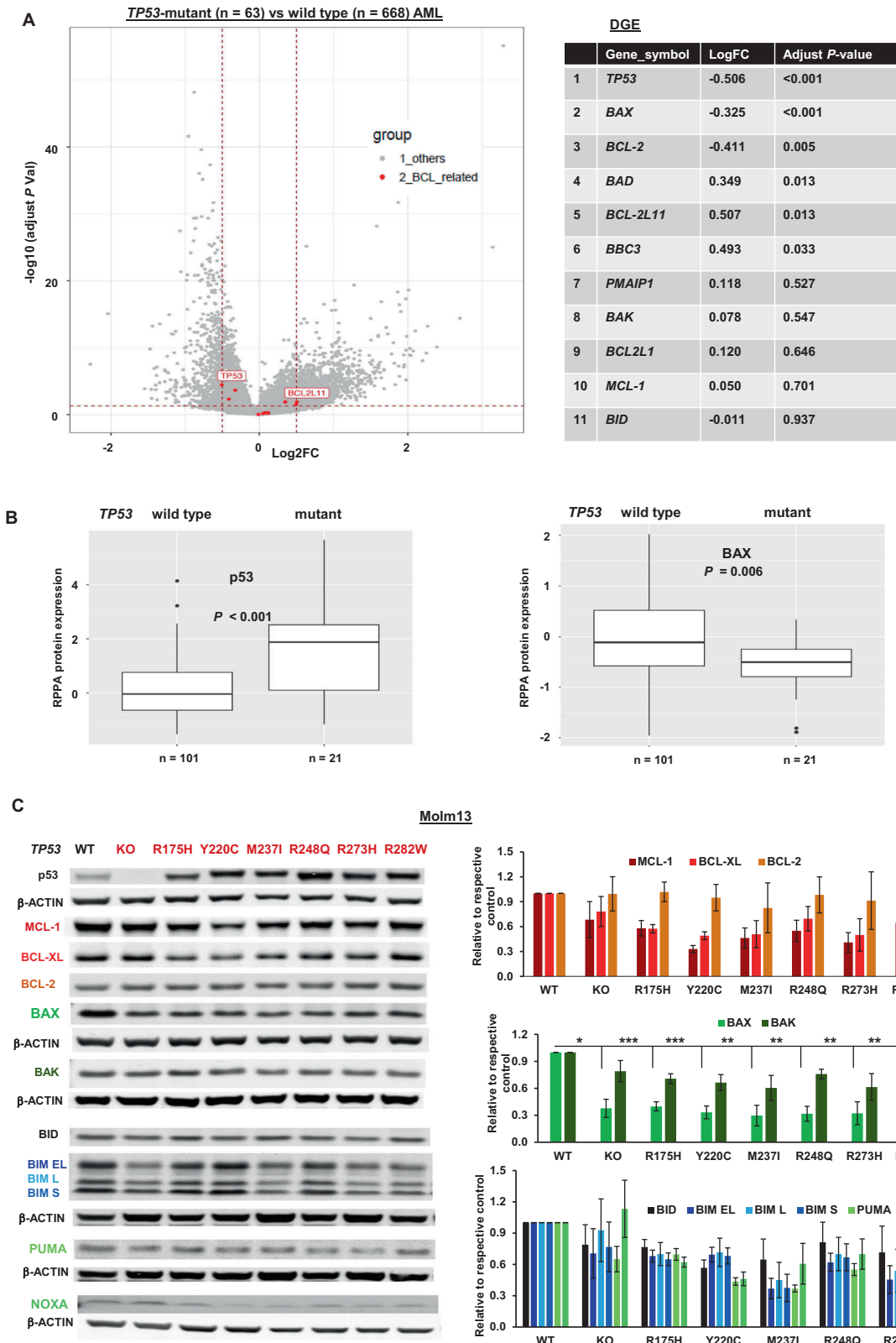
We previously reported that AML cells with acquired resistance to VEN or AMG176 expressed increased MCL-1 and BCL-2A1 and decreased BAX levels. Although VEN or AMG176 individually were less effective in these cells, the combination of the agents was highly synergistic [28]. We reported that BAX-KD diminished the sensitivity of AML cells to BH3 mimetics, but that this sensitivity was restored by the combined inhibition of BCL-2 and MCL-1 [28]. To demonstrate that BAX loss itself was sufficiently responsible for the reduced sensitivity to BH3 mimetics, we examined other BCL-2 proteins in BAX-KD cells and found that these were largely unchanged (Fig. 2A). Because BAX decrease is common in *TP53*-deficient AML cells, we tested if co-targeting BCL-2 and MCL-1 improves the responses of *TP53*-deficient cells to BH3 mimetics. We treated isogenic *TP53*-WT, -KO, and -mutant Molm13 cells with VEN, AMG176, or both. As expected, *TP53*-KO/-mutant cells exhibited decreased sensitivity to VEN or AMG176 as compared to WT controls, but when combined, the two BH3 mimetics were highly synergistic in inducing apoptosis (CI: <0.001 to 0.057) (Fig. 2B) and effectively decreased cell viability (Fig. 2C). Although less potent at lower doses in *TP53*-KO/-mutant cells than in controls, the combination at still very low concentrations (20 nM VEN/80 nM AMG176 and even 10 nM VEN/40 nM AMG176), which were essentially ineffective as single agents in *TP53*-deficient cells, were able to effectively induce apoptosis and reduce absolute cell numbers, reflected in the exceptionally low CI values, regardless of *TP53* mutational status.

Decreased BAX levels and synergism of VEN and AMG176 combination were also found in *TP53*-R248W Molm13 cells and *TP53*-KD OCI-AML3 cells (Supplemental Fig. 3A, B). The combination was also synergistic in other *TP53*-mutant leukemia cell lines (Supplemental Fig. 3C).

We found that in addition to increased MCL-1, MV4-11 cells with acquired resistance to VEN/AMG176 combination had undetectable BAX levels (Supplemental Fig. 4), further supporting the critical role of BAX in BH3 mimetic activity.

Co-targeting of BCL-2 and MCL-1 activates BAX and BAK and promotes cytochrome C release in *TP53*-mutant AML

Given that cells with a net decrease of anti-apoptotic proteins or a net increase of pro-apoptotic proteins are primed to undergo



apoptosis, we determined levels of BCL-2 family proteins in *TP53*-WT and -mutant (R175H and R248Q) Molm13 cells treated with VEN, AMG176, or the combination. As expected, AMG176 increased MCL-1 levels in all cells examined (Fig. 3A). Although it effectively induced apoptosis, the combination did not further alter the levels of BCL-2 proteins compared to those changed by

each agent alone in control or *TP53*-mutant cells. Neither agent alone, nor the combination, activated p53 in *TP53*-WT controls, in agreement with the lack of increase of BAX or NOXA.

BCL-2 family proteins cooperatively regulate apoptosis through protein-protein interaction (Fig. 3B). Using BH3 mimetic insensitive OCI-AML3 cells, we previously showed that BCL-2 inhibition

Fig. 1 BAX expression is significantly decreased in TP53-KO and -mutant AML cells. **A** Volcano plot showing differential gene expression (DGE) and the adjusted *P* values of *BCL-2* family members between *TP53*-mutant and *TP53*-WT AML cells, as assessed by RNA-seq analysis. DGE and adjusted *P* values were calculated using the limma package. *TP53* and differentially expressed *BCL-2*-related genes are highlighted in red. **B** RPPA analysis of the log₂-normalized expression levels of p53 and BAX in newly diagnosed de novo *TP53*-mutant and -WT AML. Box is 75 to 25% and bar in the middle is the median of expression. The whiskers are 95% CI, with the extremes (black dots) outside that. **C** Expression of *BCL-2* family proteins in *TP53*-KO and -mutant Molm13 cells and isogenic WT control Molm13 cells. Left, a representative Western blot; right, the relative protein expression levels quantified from three Western blots. Error bars represent the mean ± SEM of three independent experiments. Statistical analysis was performed using a Student *t*-test, and *P* < 0.05 was considered statistically significant. **P* < 0.05; ***P* < 0.01; ****P* < 0.001.

decreased *BCL-2*-BIM and *BCL-2*-BAX interactions but increased MCL-1-BIM, *BCL-XL*-BAX, and *BCL-XL*-BAK interactions; while MCL-1 inhibition decreased MCL-1-BIM interactions but increased *BCL-2*-BIM and MCL-1-BAK interactions. Only when both were inhibited, BIM, BAX, and BAK were optimally freed from anti-apoptotic *BCL-2* proteins, leading to apoptosis induction [27], supporting the notion that in BH3 mimetic less sensitive cells, modulation of multiple *BCL-2* proteins is required to effectively activate BAX/BAK and induce cell death.

We treated *TP53*-WT, -KO, and -mutant Molm13 cells with VEN, AMG176, or both and determined the levels of activated BAX, activated BAK, and cytochrome C by flow cytometry. VEN or AMG176 had a limited effect on BAX or BAK activation and cytochrome C release in *TP53*-deficient cells as compared to WT controls, whereas the combination effectively activated BAK and BAX and induced cytochrome C release (Fig. 3C). Next, we treated control and *BAX*-KD Molm13 cells. Although *BAX*-KD did not alter the levels of BAK or other *BCL-2* proteins (Fig. 2A), BAX and BAK activation and cytochrome C release were largely diminished in *BAX*-KD cells treated with VEN or AMG176. However, the combination treatment greatly induced BAX/BAK activation and cytochrome C release (Fig. 3D), supporting the highly synergistic effect of the combination in *TP53*-deficient AML cells based on this mechanism.

BH3 mimetic-driven stress response and cell death patterns are independent of *TP53* mutation status

Because combined *BCL-2* and MCL-1 inhibition can effectively activate BAX- and BAK-mediated apoptotic pathways and trigger p53-independent cell death, we reasoned that the combination would elicit similar stress responses and cell death modes irrespective of *TP53* status. Therefore, we designed a multi-parametric flow cytometry panel to concomitantly assess cell death modes (apoptosis, necroptosis, and parthanatos) and stress responses (DNA damage response, proliferation, cell cycle, autophagy, and endoplasmic reticulum [ER] stress response) utilizing dimension reduction and unsupervised clustering to gain a broad overview of the treatment-specific proteomic landscape and assess whether VEN, AMG176, or co-treatment elicited overlapping or distinct proteomic shifts across leukemia cells with different *TP53* statuses. *TP53*-WT, -KO, and -mutant (R175H and R248Q) Molm13 cells were treated with VEN, AMG176, or both. We generated a concatenated data matrix that included data points from 16 different conditions (four different types of Molm13 cells treated with DMSO, VEN, AMG176, or both) and subjected the data matrix to UMAP dimension reduction and FlowSOM clustering to partition the proteomic data into distinct subpopulations (Fig. 4A and Supplemental Fig. 5). Assessment of marker expression across the overall proteomic landscape identified live and dead cells and revealed their expression patterns (Fig. 4B, C). We identified only three live-cell subpopulations. The relatively low diversity in the live-cell compartment suggests that BH3 mimetics did not induce a divergent stress response characterized by the emergence of distinct subpopulations with distinct stress patterns. Indeed, the overall proteomic architectures of leukemia cells exposed to drug combinations overlapped. We observed that VEN, AMG176, or co-treatment did not drive the emergence of distinct subsets that

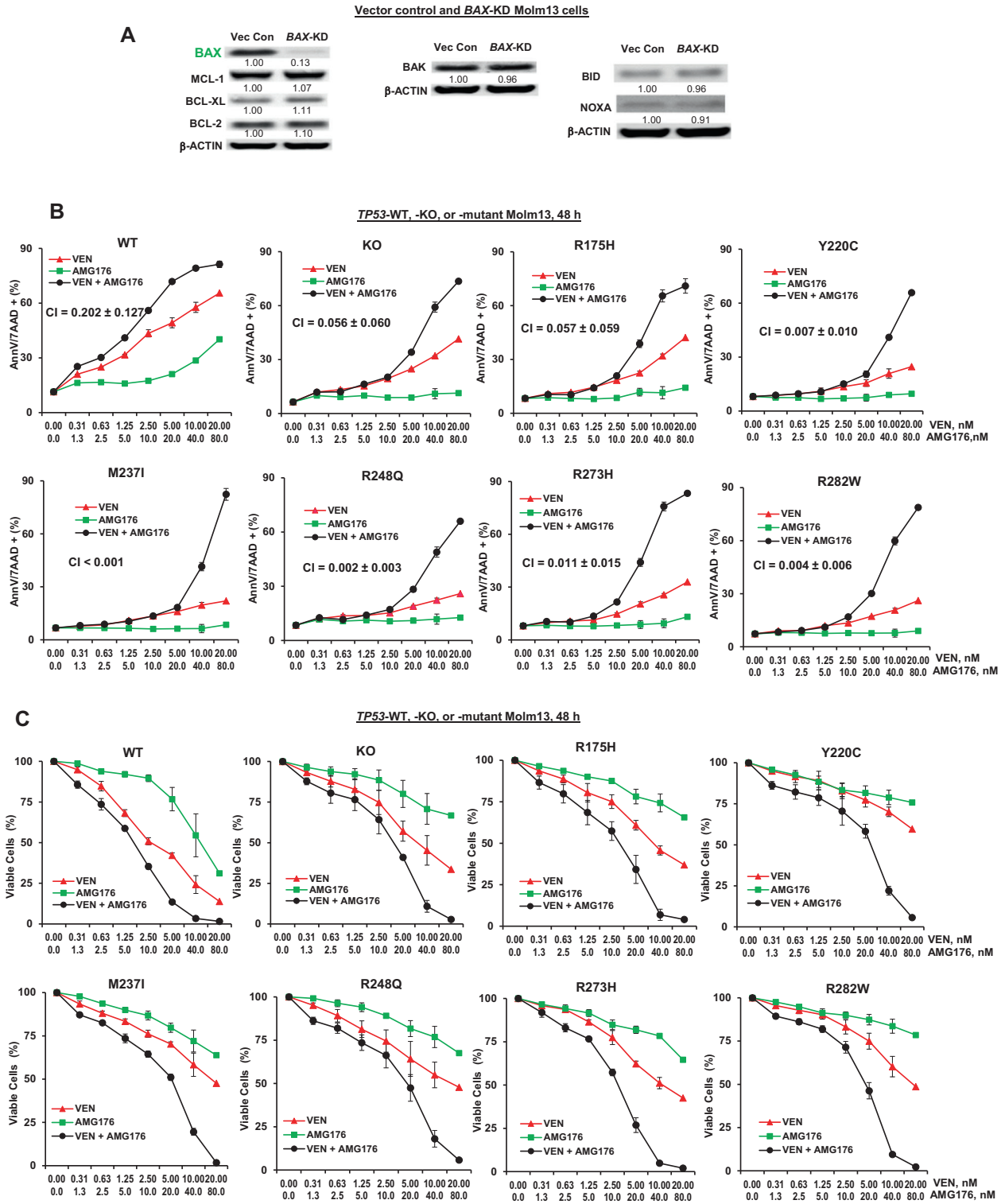
were not present in controls (Supplemental Fig. 5). Thus, we concluded that BH3 mimetics do not induce autophagy, ER stress, or a DNA damage response nor alter the proliferation status of leukemia cells. A lack of DNA damage and stable RIP3 expression in surviving cells ruled out parthanatos and necroptosis [42] as mechanisms of cell death upon treatment with BH3 mimetics (Fig. 4B). Assessment of the dead cell compartment revealed distinct, hierarchically organized layers of cell death (Fig. 4A, B) and caspase 3 activation and cleaved-PARP, indicating that apoptosis is the main mechanism of cell death induced by BH3 mimetics [41].

To assess whether *TP53* status alters cell death patterns and stress responses in an unsupervised manner, we quantified the fractions of leukemia cell subpopulations with different *TP53* backgrounds treated with VEN, AMG176, or both (Fig. 4D) and performed clustering analysis using the frequencies of subpopulations detected across the overall leukemia landscape to delineate the direction of the treatment response and identify the similarity of cluster composition and thus response patterns among the isogenic cells with different *TP53* statuses. We found that *TP53*-WT, -KO, and -mutant cells treated with the same drug regimen were positioned in proximity on high-dimensional space and clustered together (Fig. 4E), indicating that *TP53* status does not affect BH3 mimetic-driven stress response and cell death patterns. AMG176 alone did not induce significant cell death or a stress response; therefore, AMG176-treated cells clustered together with controls. The clustering was mainly driven by treatments, rather than *TP53* status. Leukemia cells treated with VEN alone, although less effective, were clustered together in close proximity with VEN plus AMG176-treated cells (Fig. 4E). These findings indicate that leukemia cells from distinct *TP53* backgrounds have an overlapping overall response landscape following treatment with BH3 mimetics and thus provide a rationale for using BH3 mimetics targeting both *BCL-2* and MCL-1 to effectively treat *TP53*-deficient and -mutant leukemia cells.

Lastly, we selected the live cells and assessed their proteomic profiles across different conditions (Fig. 4F and Supplemental Fig. 5) to gain insights into the survival mechanisms. We observed that *TP53*-WT, -KO, or -mutant Molm13 cells with high levels of autophagy and ER stress preferentially survived after treatment with BH3 mimetics, particularly VEN alone and VEN plus AMG176 (Fig. 4F). In general, proliferating leukemia cells are more susceptible to chemotherapeutic agents or a variety of targeted therapies, but we observed that proliferating cells were preferentially enriched after treatment with BH3 mimetics, particularly VEN and VEN/AMG176 combination (Fig. 4F, G). Results suggest that proliferating cells could be less sensitive to individual BH3 mimetics, particularly to VEN (Fig. 4F). However, VEN/AMG176 combination substantially decreased the fractions of proliferating cells that would survive with VEN alone. This notion could be exploited by modulating the proliferation status of leukemia cells to render them more susceptible to BH3 mimetics.

Combined *BCL-2* and MCL-1 inhibition is effective against *TP53*-mutant AML cells and stem/progenitor cells

To validate the potential clinical relevance of targeting *BCL-2* and MCL-1 in *TP53*-mutant AML mimicking a microenvironment setting in vitro, we co-cultured cells from eight AML patients



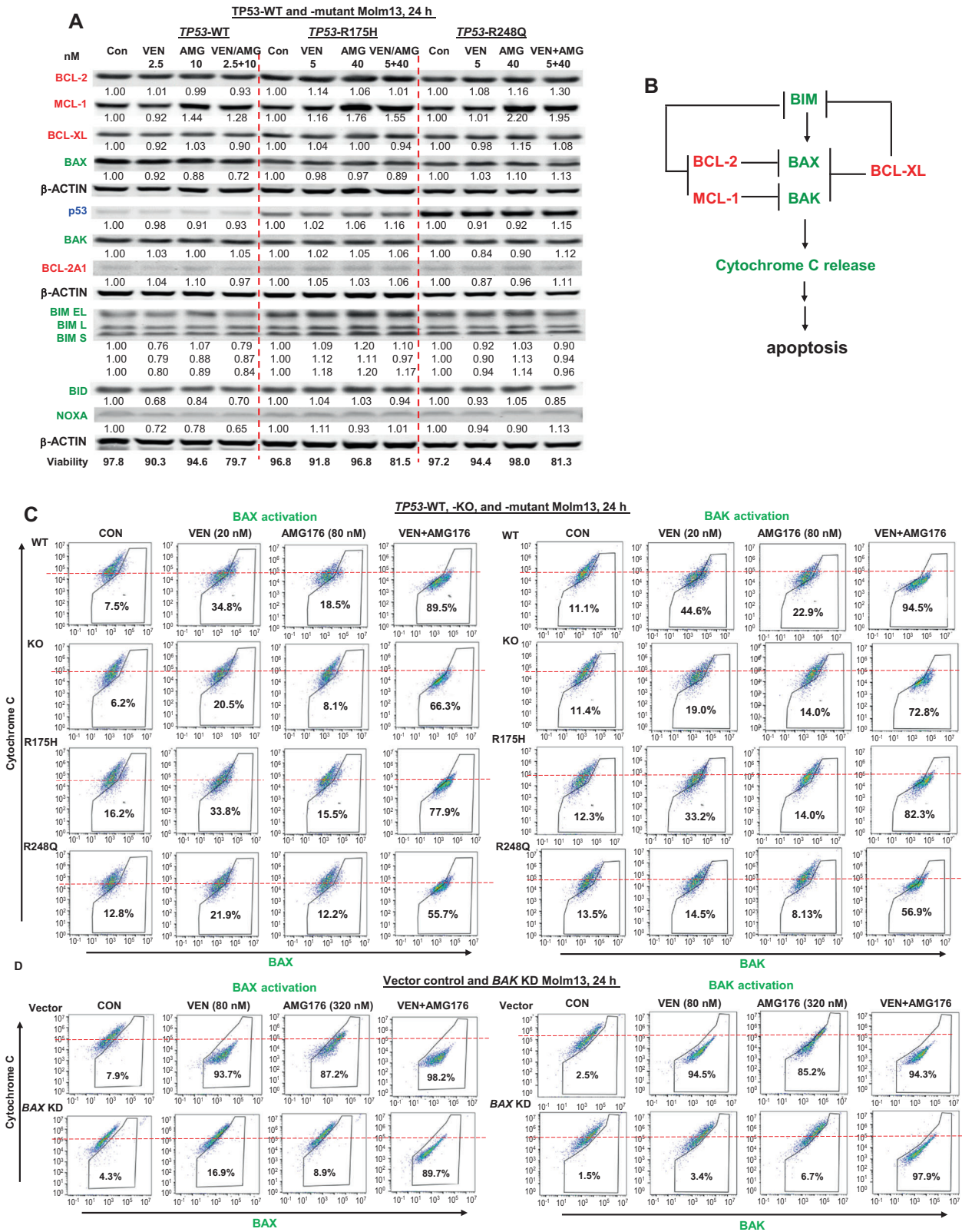
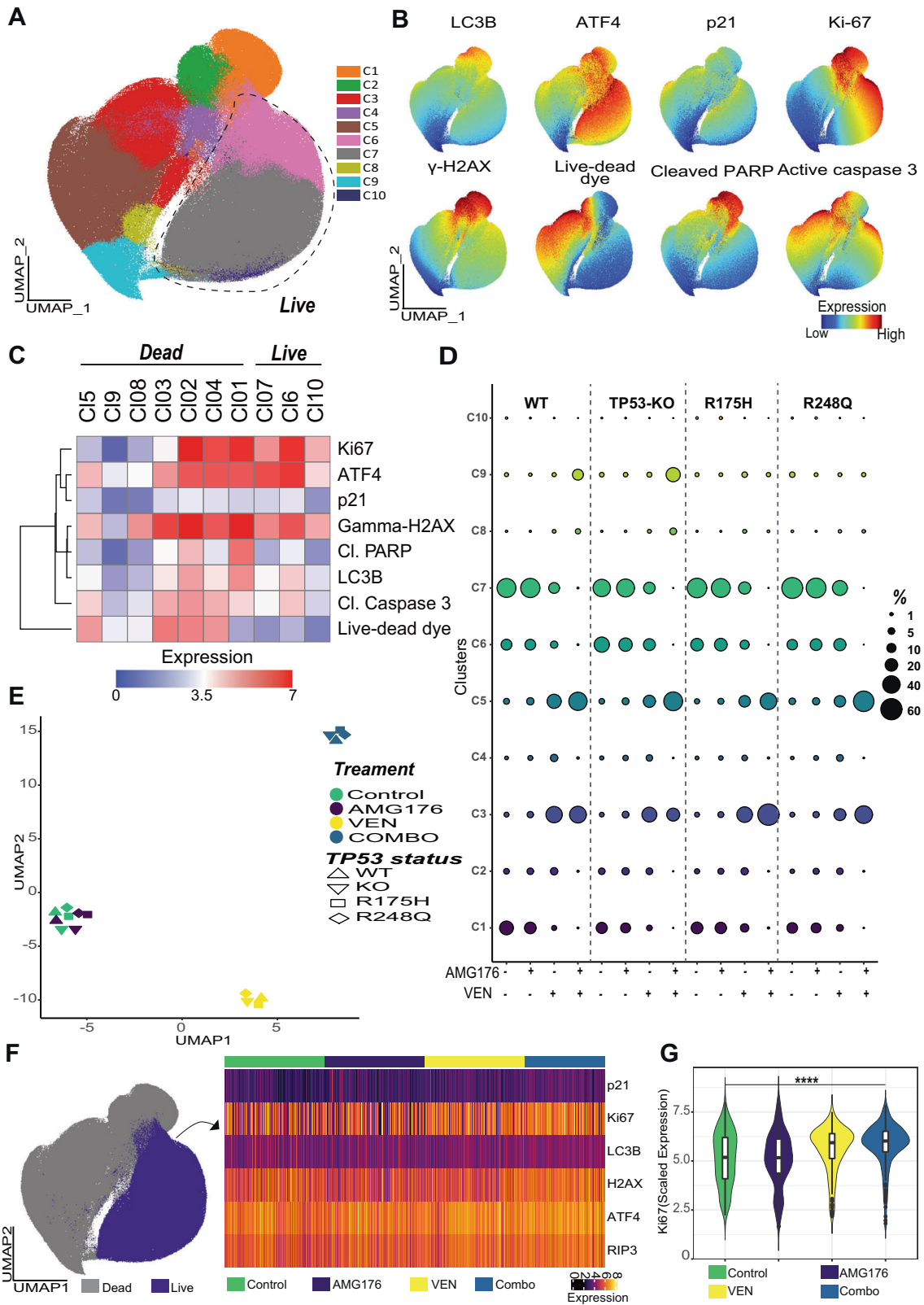


Fig. 3 The role of BCL-2 family members in BH3 mimetic-induced apoptosis. **A** TP53-WT and -mutant (R175H and R248Q) Molm13 cells were treated with VEN, AMG176 (AMG), or both at the indicated concentrations for 24 h. Protein levels were determined by Western blot analysis. **B** Schematic of apoptosis induction requiring BAX and BAK activation, which is activated by BIM and blocked by BCL-2 and MCL-1. **C, D** TP53-WT, -KO, or -mutant Molm13 cells (**C**) and vector control or BAX-KD Molm13 cells (**D**) were treated with VEN, AMG176, or both at the indicated concentrations for 24 h. BAX and BAK activation and cytochrome C release were measured by flow cytometry. h hour.



with *TP53* mutations (6/8 had co-mutations, 5/8 were resistant to VEN-based therapy) (Table 1) with MSCs and treated them with VEN, AMG176, or both. In both leukemia blasts and stem/progenitor cells, the combination of VEN (5 nM) and AMG176 (125 nM) induced significantly more cell death (Fig. 5A) and

reduced cell viability (Fig. 5B) compared with either agent alone. The combination of synergistically induced cell death in both CD45⁺ leukemia blasts and CD34⁺ stem/progenitor cells (Fig. 5C, patients #26 and #28). The CI values of all eight patient samples in leukemia blasts (0.04 ± 0.04 to 0.34 ± 0.10) and stem/progenitor

Fig. 4 The combination of VEN and AMG176 induces similar cell death and stress patterns in *TP53*-WT, -KO, and -mutant AML cells. **A** *TP53*-WT, -KO, and -mutant (R175H and R248Q) Molm13 cells were treated with DMSO control, VEN, AMG176, or VEN plus AMG176, stained with an array of antibodies, and subjected to flow cytometry. Cells were then subjected to UMAP dimension reduction and projected on two-dimensional plots. The FlowSOM algorithm was utilized for automated cell population identification; the colors indicate FlowSOM clusters. **B** The UMAP plots for the indicated markers; the colors indicate marker expression intensity. **C** Heatmap of the arcsine-transformed expression intensities of the markers used for dimension reduction and clustering across the FlowSOM clusters shown in panel **B**. Live and dead cell clusters were identified based on the marker expression patterns shown in panel **B**. **D** Bubble plot of the frequencies of the FlowSOM clusters shown in panel **A** across *TP53*-WT, -KO, and -mutant (R175H and R248Q) Molm13 cells treated with control, VEN, AMG176, or VEN plus AMG176. **E** UMAP plot of the differential responses to treatment with control, VEN, AMG176, or VEN plus AMG176. The FlowSOM cluster frequencies shown in panel **C** were used for dimension reduction. **F** UMAP map of live cells (purple) and dead cells (gray) and heatmap of the expressions of the selected markers. **G** Violin plot of scaled Ki-67 signal intensities of *TP53*-WT, KO, and mutant leukemia cells and cells exposed to VEN, AMG176, or VEN plus AMG176 for 48 h. Live cells were selected for plotting and 200 cells (50 cells each of *TP53*-WT, KO, R175H, and R248Q) from each condition (control, AMG176, VEN, and combo) were shown. CI cleaved, combo combination.

cells (0.07 ± 0.08 to 0.28 ± 0.14) are shown in Supplemental Table 1. Data indicate that the combinatorial therapy of BCL-2 and MCL-1 inhibition is highly effective even in the presence of MSCs.

Combined inhibition of BCL-2 and MCL-1 is highly effective in vivo in a *TP53*-WT/*TP53*-R248W Molm13 xenograft model

To assess the therapeutic potential of co-targeting BCL-2 and MCL-1 in vivo and mimic the clinical scenario, we performed experiments using xenografts of luciferase/GFP-labeled *TP53*-WT and BFP-labeled *TP53*-R248W Molm13 cell mixtures (10:1) in NSG mice (Fig. 6A). In vivo imaging analysis showed that the combination treatment significantly decreased *TP53*-WT Molm13 compared to the control or either BH3 mimetic alone at weeks-1 and -2 (Fig. 6B). At week-3, none of the controls and only one AMG176-treated mouse was alive; the combination was more effective than VEN alone. To distinguish the effects of treatments on *TP53*-WT and -mutant leukemia cells, we measured circulating GFP (*TP53*-WT)- and BFP (*TP53*-R248W)-labeled cells by flow cytometry. VEN or AMG176 alone had minimal effects on either *TP53*-WT or *TP53*-R248W Molm13 cells, and their combination significantly reduced both cell types (Fig. 6C). There was little difference between the median survival duration of control mice (23 days) and that of AMG176-treated (24.5 days) or VEN-treated mice (25 days). The median survival duration of the combination-treated mice (45 days) was significantly longer than those of the control, VEN-, and AMG176-treated mice ($P = 0.001$ for all three comparisons) (Fig. 6D).

DISCUSSION

We demonstrate that the significant reduction of BAX is critical for the decreased sensitivity of *TP53*-mutant AML to individual BH3 mimetics targeting BCL-2 or MCL-1. The combined inhibition of both effectively activates BAX and synergistically decreases cell viability primarily by apoptosis induction in AML cells largely independent of *TP53* mutational status. Hence, the diminished activity of BH3 mimetics in *TP53*-defective cells can be circumvented in a p53-independent manner by co-targeting BCL-2 and MCL-1.

CRISPR genome editing analyses have demonstrated that the loss of WT *TP53* or p53-regulated apoptosis regulators, such as BAX, confers VEN resistance [18]. BAX mutations have been identified as a mechanism of BH3 mimetic resistance in AML [29]. BAX mutations have also been detected in the myeloid compartment of CLL patients with clonal hematopoiesis who were treated with VEN [46], which further supports the notion that BAX has a critical role in BH3 mimetic-induced death of myeloid leukemia cells. In the present study, we found significantly decreased expression levels of BAX in *TP53*-mutant patient samples and

isogenic AML cells compared to *TP53*-WT AML cells. We also found that genetic silencing of BAX rendered AML cells resistant to BH3 mimetics [28] and that BAX is largely undetectable in AML cells with acquired resistance to both VEN and AMG176. Furthermore, *TP53*-deficiency or BAX-KD alone sufficiently inhibits BAX and BAK activation. Collectively, these findings show that the reduction or loss of BAX are critical for BH3 mimetic resistance and contributes to the vastly reduced activity of BH3 mimetics in *TP53*-mutant AML.

Following exposure to chemotherapeutic agents, *TP53*-mutant clones are commonly selected and frequently become dominant, conferring further resistance to other therapies [47, 48]. Although efforts have been made to target selected *TP53*-mutants [49, 50], these approaches have limited clinical applicability, as >100 *TP53* mutations have been identified in AML [25]. We here demonstrate that the combined inhibition of BCL-2 and MCL-1 circumvents the resistance in *TP53*-deleted or mutant-AML to individual BH3 mimetics and synergistically induces *TP53*-independent profound apoptosis in AML cells and AML stem/progenitor cells in vitro and in vivo. Hence, our approach has potentially broad clinical implications, beyond approaches targeting selective *TP53* mutations.

Despite effectiveness, the combined inhibition of BCL-2 and MCL-1 was less robust in *TP53*-deficient/-mutant than in *TP53*-WT AML. Achieving efficacies in *TP53*-deficient/-mutant AML that were similar to that in WT AML required higher doses of both agents. Nevertheless, xenograft-bearing mice with *TP53*-mutant AML cells under combination treatment survived almost twice as long than those treated with either agent alone using the same dose and treatment schedule as we previously described, in which a VEN/HMA resistant *TP53*-WT PDX model showed a three-fold survival extension [28]. AMG176 and VEN/AMG176 clinical trials in hematological malignancies have been initiated. Careful titration of the doses of each BH3 mimetic to maximize the combination's efficacy and minimize toxicity will hopefully result in an effective and safe combinatorial regimen.

Besides direct inhibition, indirect targeting MCL-1 through mechanisms such as inhibition of MAPK or CDK9 could also sensitize AML cells to VEN. Given the critical role of BAX in mitochondria-regulated apoptosis, pharmacologically or genetically increasing BAX levels may improve the lethality of BH3 mimetics and benefit patients whose disease is resistant to BH3 mimetics. In fact, with an improved understanding of the structure-function relationship of BAX, researchers are developing strategies to modulate BAX activity or expression with various approaches, including small molecules and peptides [51]. All approaches that increase pro- and decrease anti-apoptotic BCL-2 have the potential to sensitize *TP53*-mutant AML cells to VEN and warrant further exploration.

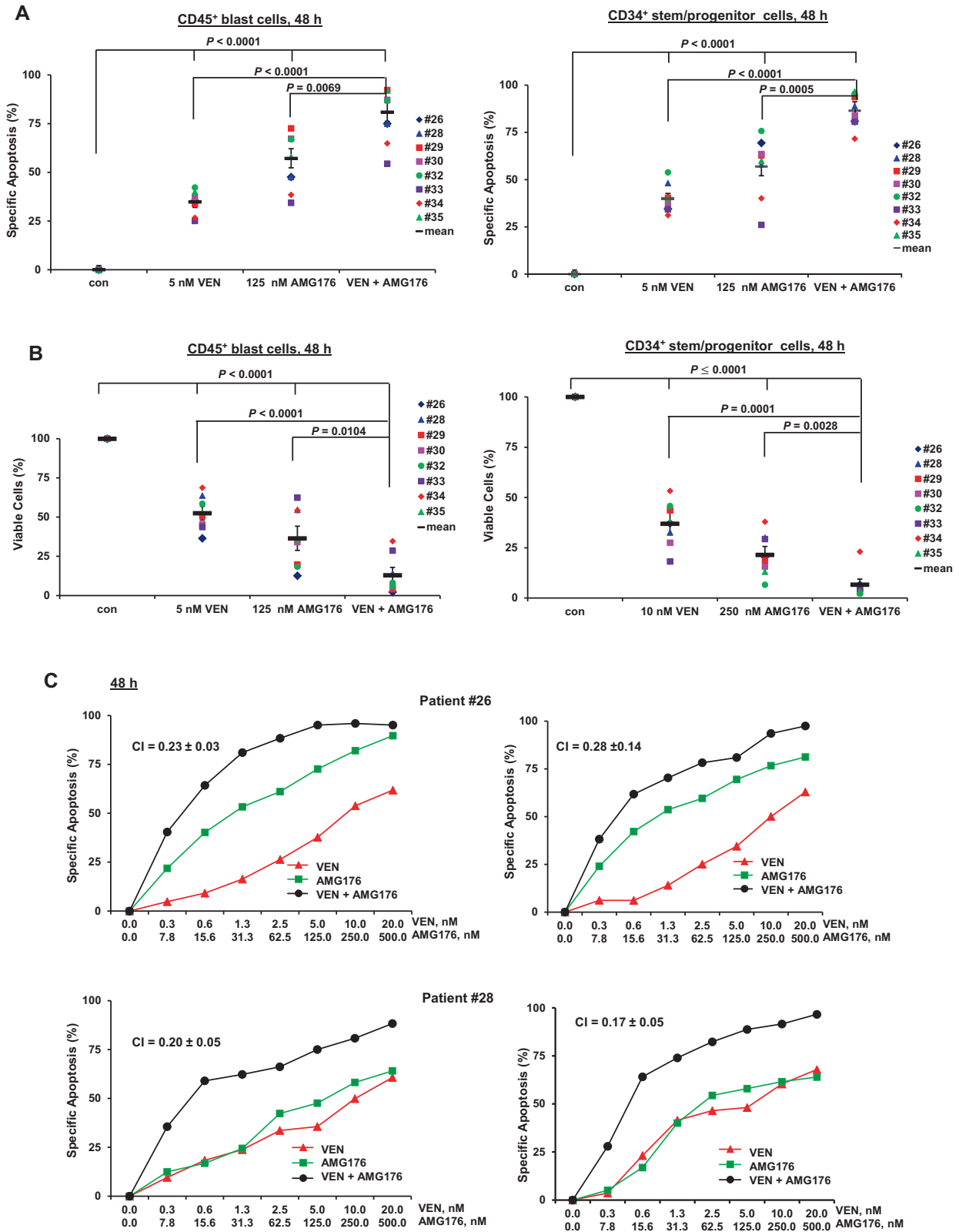


Fig. 5 The combined inhibition of BCL-2 and MCL-1 is significantly more effective in AML cells and AML stem/progenitor cells from patients with TP53 mutations. **A, B** AML patient samples ($n = 8$) with TP53 mutations were treated with VEN, AMG176, or both for 48 h. Apoptosis (**A**) and viable cells (**B**) were determined by flow cytometry. h hour. Error bars represent mean \pm SEM of data from individual patients. **C** AML patient samples ($n = 8$) with TP53 mutations were treated with various concentrations of VEN, AMG176, or both for 48 h. Apoptosis and the CI values from two representative patient samples (#26, #28) are shown. Cell death is expressed as specific apoptosis and viable cells are expressed as % compared to the control of 100%. con control.

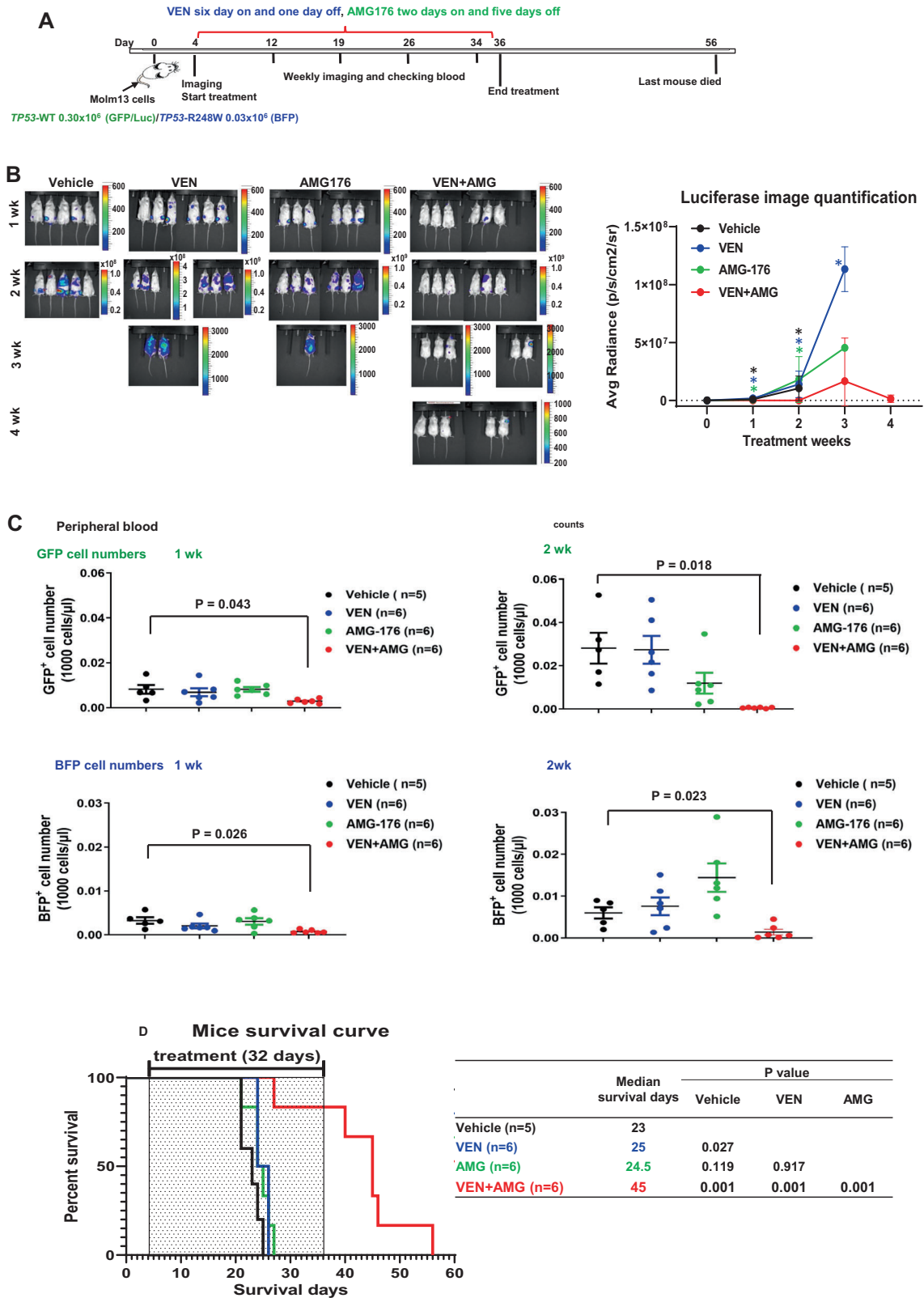


Fig. 6 The combined inhibition of BCL-2 and MCL-1 exhibits stronger *in vivo* anti-leukemia activity in a xenograft mouse model. **A** Experimental scheme. **B** Bioluminescence imaging and quantification. **C** Circulating numbers of GFP⁺ and BFP⁺ cells after week 1 (left) and week 2 (right) of treatment as determined by flow cytometry. **D** Survival. $n = 5$ or 6 /group. AMG AMG176, wk week. Error bars represent the mean \pm SD of data from individual mice.

DATA AVAILABILITY

Materials described in the manuscript, including all relevant raw data, will be freely available to any researcher wishing to use them for non-commercial purposes, without breaching participant confidentiality.

REFERENCES

- Christiansen DH, Andersen MK, Pedersen-Bjergaard J. Mutations with loss of heterozygosity of p53 are common in therapy-related myelodysplasia and acute myeloid leukemia after exposure to alkylating agents and significantly associated with deletion or loss of 5q, a complex karyotype, and a poor prognosis. *J Clin Oncol*. 2001;19:1405–13.
- Ok CY, Patel KP, Garcia-Manero G, Routbort MJ, Fu B, Tang G, et al. Mutational profiling of therapy-related myelodysplastic syndromes and acute myeloid leukemia by next generation sequencing, a comparison with de novo diseases. *Leuk Res*. 2015;39:348–54.
- Pedersen-Bjergaard J, Andersen MK, Andersen MT, Christiansen DH. Genetics of therapy-related myelodysplasia and acute myeloid leukemia. *Leukemia* 2008;22:240–8.
- Rücker FG, Schlenk RF, Bullinger L, Kayser S, Teleanu V, Kett H, et al. TP53 alterations in acute myeloid leukemia with complex karyotype correlate with specific copy number alterations, monosomal karyotype, and dismal outcome. *Blood* 2012;119:2114–21.
- Hou HA, Chou WC, Kuo YY, Liu CY, Lin LI, Tseng MH, et al. TP53 mutations in de novo acute myeloid leukemia patients: longitudinal follow-ups show the mutation is stable during disease evolution. *Blood Cancer J*. 2015;5:e331.
- Stengel A, Kern W, Haferlach T, Meggendorfer M, Fasan A, Haferlach C. The impact of TP53 mutations and TP53 deletions on survival varies between AML, ALL, MDS and CLL: an analysis of 3307 cases. *Leukemia* 2017;31:705–11.
- Kadia TM, Jain P, Ravandi F, Garcia-Manero G, Andreeff M, Takahashi K, et al. TP53 mutations in newly diagnosed acute myeloid leukemia: Clinicomolecular characteristics, response to therapy, and outcomes. *Cancer* 2016;122:3484–91.
- Short NJ, Montalban-Bravo G, Hwang H, Ning J, Franquiz MJ, Kanagal-Shamanna R, et al. Prognostic and therapeutic impacts of mutant TP53 variant allelic frequency in newly diagnosed acute myeloid leukemia. *Blood Adv*. 2020;4:5681–9.
- DiNardo CD, Pratz K, Pullarkat V, Jonas BA, Arellano M, Becker PS, et al. Venetoclax combined with decitabine or azacitidine in treatment-naïve, elderly patients with acute myeloid leukemia. *Blood*. 2019;133:7–17.
- DiNardo CD, Pratz KW, Letai A, Jonas BA, Wei AH, Thirman M, et al. Safety and preliminary efficacy of venetoclax with decitabine or azacitidine in elderly patients with previously untreated acute myeloid leukaemia: a non-randomised, open-label, phase 1b study. *Lancet Oncol*. 2018;19:216–28.
- Alldoss I, Yang D, Aribi A, Ali H, Sandhu K, Al Malki MM, et al. Efficacy of the combination of venetoclax and hypomethylating agents in relapsed/refractory acute myeloid leukemia. *Haematologica*. 2018;103:e404–7.
- Joergers AC, Fersht AR. The tumor suppressor p53: from structures to drug discovery. *Cold Spring Harb Perspect Biol*. 2010;2:a000919.
- DiNardo CD, Tiong IS, Quaglieri A, MacRaild S, Loghavi S, Brown FC, et al. Molecular patterns of response and treatment failure after frontline venetoclax combinations in older patients with AML. *Blood*. 2020;135:791–803.
- Kim K, Maiti A, Loghavi S, Pourebrahimi R, Kadia TM, Rausch CR, et al. Outcomes of TP53-mutant acute myeloid leukemia with decitabine and venetoclax. *Cancer*. 2021;133:3689.
- Stahl M, Menghrajani K, Derkach A, Chan A, Xiao W, Glass J, et al. Clinical and molecular predictors of response and survival following venetoclax therapy in relapsed/refractory AML. *Blood Adv*. 2021;5:1552–64.
- Wang YW, Tsai CH, Lin CC, Tien FM, Chen YW, Lin HY, et al. Cytogenetics and mutations could predict outcome in relapsed and refractory acute myeloid leukemia patients receiving BCL-2 inhibitor venetoclax. *Ann Hematol*. 2020;99:501–11.
- Schimmer R, Kovtonyuk LV, Klemm N, Fullin J, Stolz SM, Mueller J, et al. TP53 mutations confer resistance to hypomethylating agents and BCL-2 inhibition in myeloid neoplasms. *Blood Adv*. 2022;6:3201–6.
- Nechiporuk T, Kurtz SE, Nikolova O, Liu T, Jones CL, D'Alessandro A, et al. The TP53 apoptotic network is a primary mediator of resistance to BCL2 inhibition in AML cells. *Cancer Discov*. 2019;9:910–25.
- Venugopal S, Shoukier M, Konopleva M, Dinardo CD, Ravandi F, Short NJ, et al. Outcomes in patients with newly diagnosed TP53-mutated acute myeloid leukemia with or without venetoclax-based therapy. *Cancer*. 2021;127:3541–51.
- Pan R, Hogdal LJ, Benito JM, Bucci D, Han L, Borthakur G, et al. Selective BCL-2 inhibition by ABT-199 causes on-target cell death in acute myeloid leukemia. *Cancer Discov*. 2014;4:362–75.
- Pan R, Ruvolo V, Mu H, Levenson JD, Nichols G, Reed JC, et al. Synthetic lethality of combined Bcl-2 inhibition and p53 activation in AML: mechanisms and superior antileukemic efficacy. *Cancer Cell*. 2017;32:748–60. e6
- Wang X, Mak PY, Mu H, Tao W, Rao A, Visweswaran R, et al. Combinatorial inhibition of focal adhesion kinase and BCL-2 enhances antileukemia activity of venetoclax in acute myeloid leukemia. *Mol Cancer Ther*. 2020;19:1636–48.
- Blombery P, Anderson MA, Gong JN, Thijssen R, Birkinshaw RW, Thompson ER, et al. Acquisition of the recurrent Gly101Val mutation in BCL2 confers resistance to venetoclax in patients with progressive chronic lymphocytic leukemia. *Cancer Discov*. 2019;9:342–53.
- Caenepeel S, Brown SP, Belmontes B, Moody G, Keegan KS, Chui D, et al. AMG 176, a selective MCL1 inhibitor, is effective in hematologic cancer models alone and in combination with established therapies. *Cancer Discov*. 2018;8:1582–97.
- Dutta S, Pregartner G, Rücker FG, Heitzer E, Zebisch A, Bullinger L, et al. Functional classification of TP53 mutations in acute myeloid leukemia. *Cancers* 2020;12:637.
- Chen X, Glytsou C, Zhou H, Narang S, Reyna DE, Lopez A, et al. Targeting mitochondrial structure sensitizes acute myeloid leukemia to venetoclax treatment. *Cancer Discov*. 2019;9:890–909.
- Carter BZ, Mak PY, Tao W, Warmoes M, Lorenzi PL, Mak D, et al. Targeting MCL-1 dysregulates cell metabolism and leukemia-stroma interactions and resensitizes acute myeloid leukemia to BCL-2 inhibition. *Haematologica*. 2020;23:260331.
- Carter BZ, Mak PY, Tao W, Zhang Q, Ruvolo V, Kuruvilla VM, et al. Maximal activation of apoptosis signaling by cotargeting antiapoptotic proteins in BH3 mimetic-resistant AML and AML stem cells. *Mol Cancer Ther*. 2022;21:879–89.
- Moujalled DM, Brown FC, Chua CC, Dengler MA, Pomilio G, Anstee NS, et al. Acquired mutations in BAX confer resistance to BH3-mimetic therapy in acute myeloid leukemia. *Blood*. 2023;141:634–44.
- Romano P, Manniello A, Aresu O, Armento M, Cesaro M, Parodi B. Cell line data base: structure and recent improvements towards molecular authentication of human cell lines. *Nucleic Acids Res*. 2009;37:D925–32.
- Nishida Y, Montoya RH, Morita K, Tanaka T, Wang F, Takahashi K, et al. Clonal expansion of mutant p53 clones by MDM2 inhibition in acute myeloid leukemias. *Blood*. 2020;136:27–8.
- Boettcher S, Miller PG, Sharma R, McConkey M, Leventhal M, Krivtsov AV, et al. A dominant-negative effect drives selection of TP53 missense mutations in myeloid malignancies. *Science*. 2019;365:599–604.
- Kojima K, Duvvuri S, Ruvolo V, Samaniego F, Younes A, Andreeff M. Decreased sensitivity of 17p-deleted chronic lymphocytic leukemia cells to a small molecule BCL-2 antagonist ABT-737. *Cancer*. 2012;118:1023–31.
- Carter BZ, Mak DH, Schober WD, Dietrich MF, Pinilla C, Vassilev LT, et al. Triptolide sensitizes AML cells to TRAIL-induced apoptosis via decrease of XIAP and p53-mediated increase of DR5. *Blood*. 2008;111:3742–50.
- Studeniy M, Marini FC, Champlin RE, Zompetta C, Fidler IJ, Andreeff M. Bone marrow-derived mesenchymal stem cells as vehicles for interferon-beta delivery into tumors. *Cancer Res*. 2002;62:3603–8.
- Carter BZ, Qiu YH, Zhang N, Coombes KR, Mak DH, Thomas DA, et al. Expression of ARC (apoptosis repressor with caspase recruitment domain), an antiapoptotic protein, is strongly prognostic in AML. *Blood*. 2011;117:780–7.
- Kornblau SM, Tibes R, Qiu YH, Chen W, Kantarjian HM, Andreeff M, et al. Functional proteomic profiling of AML predicts response and survival. *Blood*. 2009;113:154–64.
- Tibes R, Qiu Y, Lu Y, Hennessy B, Andreeff M, Mills GB, et al. Reverse phase protein array: validation of a novel proteomic technology and utility for analysis of primary leukemia specimens and hematopoietic stem cells. *Mol Cancer Ther*. 2006;5:2512–21.
- Carter BZ, Mak PY, Mu H, Zhou H, Mak DH, Schober W, et al. Combined targeting of BCL-2 and BCR-ABL tyrosine kinase eradicates chronic myeloid leukemia stem cells. *Sci Transl Med*. 2016;8:355ra117.
- Thijssen R, Diepstraten ST, Moujalled D, Chew E, Flensburg C, Shi MX, et al. Intact TP-53 function is essential for sustaining durable responses to BH3-mimetic drugs in leukemias. *Blood*. 2021;137:2721–35.
- Muftuoglu M, Mak PY, Ruvolo V, Nishida Y, Ruvolo PP, Carter BZ, et al. High dimensional interrogation of stress response patterns and cell death modes in AML. *Blood*. 2020;136:15.
- Bergamaschi D, Vossenkamper A, Lee WYJ, Wang P, Bochukova E, Warnes G. Simultaneous polychromatic flow cytometric detection of multiple forms of regulated cell death. *Apoptosis* 2019;24:453–64.
- Muftuoglu M, Li L, Liang S, Mak D, Lin AJ, Fang J, et al. Extended live-cell barcoding approach for multiplexed mass cytometry. *Sci Rep*. 2021;11:12388.
- Butler A, Hoffman P, Smibert P, Papalexis E, Satija R. Integrating single-cell transcriptomic data across different conditions, technologies, and species. *Nat Biotechnol*. 2018;36:411–20.
- Chou TC, Talalay P. Quantitative analysis of dose-effect relationships: the combined effects of multiple drugs or enzyme inhibitors. *Adv Enzym Regul*. 1984;22:27–55.

46. Blombery P, Lew TE, Dengler MA, Thompson ER, Lin VS, Chen X, et al. Clonal hematopoiesis, myeloid disorders and BAX-mutated myelopoiesis in patients receiving venetoclax for CLL. *Blood*. 2022;139:1198–207.
47. Wong TN, Ramsingh G, Young AL, Miller CA, Touma W, Welch JS, et al. Role of TP53 mutations in the origin and evolution of therapy-related acute myeloid leukaemia. *Nature*. 2015;518:552–5.
48. Yan B, Chen Q, Shimada K, Tang M, Li H, Gurumurthy A, et al. Histone deacetylase inhibitor targets CD123/CD47-positive cells and reverse chemoresistance phenotype in acute myeloid leukemia. *Leukemia*. 2019;33:931–44.
49. Chen S, Wu JL, Liang Y, Tang YG, Song HX, Wu LL, et al. Arsenic trioxide rescues structural p53 mutations through a cryptic allosteric site. *Cancer Cell*. 2021;39:225–39.
50. Hsiue EH, Wright KM, Douglass J, Hwang MS, Mog BJ, Pearlman AH, et al. Targeting a neoantigen derived from a common TP53 mutation. *Science*. 2021;371:1.
51. Spitz AZ, Gavathiotis E. Physiological and pharmacological modulation of BAX. *Trends Pharm Sci*. 2022;43:206–20.

ACKNOWLEDGEMENTS

This work was supported in part by MD Anderson Moonshot funding; the National Institutes of Health through MD Anderson's Cancer Center Support Grant (P30CA016672) of Flow Cytometry/Image Core; and the Paul and Mary Haas Chair in Genetics (to M.A.). We thank the Torsten Haferlach Leukemia Diagnostic Foundation for providing gene expression data. We also thank Joe Munch in MD Anderson's Research Medical Library for editing and Deanna Alexander for assisting with submitting the manuscript. EA is a TRIUMPH Fellow in the CPRIT Training Program (RP210028).

AUTHOR CONTRIBUTIONS

BZC conceptualized the study, analyzed data, and wrote the manuscript; PYM, WT, EA, LBO, XH, SL, SB, YN, VR, PEH, PKM, TH, SK, and MM performed experiments and/or analyzed data or provided materials/data, and edited the manuscript; MA conceptualized the study, interpreted the data, and edited the manuscript.

CONFLICT OF INTEREST

PEH and PKM are employees of Amgen.

ADDITIONAL INFORMATION

Supplementary information The online version contains supplementary material available at <https://doi.org/10.1038/s41408-023-00830-w>.

Correspondence and requests for materials should be addressed to Bing Z. Carter or Michael Andreeff.

Reprints and permission information is available at <http://www.nature.com/reprints>

Publisher's note Springer Nature remains neutral with regard to jurisdictional claims in published maps and institutional affiliations.



Open Access This article is licensed under a Creative Commons Attribution 4.0 International License, which permits use, sharing, adaptation, distribution and reproduction in any medium or format, as long as you give appropriate credit to the original author(s) and the source, provide a link to the Creative Commons license, and indicate if changes were made. The images or other third party material in this article are included in the article's Creative Commons license, unless indicated otherwise in a credit line to the material. If material is not included in the article's Creative Commons license and your intended use is not permitted by statutory regulation or exceeds the permitted use, you will need to obtain permission directly from the copyright holder. To view a copy of this license, visit <http://creativecommons.org/licenses/by/4.0/>.

© The Author(s) 2023, corrected publication 2023